

## Kinetic Analysis of Excimer Emission of Vinyl-naphthalene–Styrene Copolymers

Shinzaburo ITO, Masahide YAMAMOTO, and Yasunori NISHIJIMA

*Department of Polymer Chemistry, Kyoto University,  
Sakyo-ku, Kyoto 606, Japan.*

(Received February 26, 1981)

**ABSTRACT:** The photoluminescence characteristics of 2-vinylnaphthalene–styrene copolymers were studied under photostationary and transient conditions. Kinetic analysis of the monomer and the excimer emission was carried out, where the migration rate of excitation energy  $k_t$  and the excimer formation rate of an adjacent pair of naphthalene units on the copolymer chain  $k_{21}$  were treated. Observed decay curves and quantum yields were in agreement with those calculated by the kinetic equations, and the rate constants were obtained:  $k_t = 3 \times 10^8 \text{ s}^{-1}$ ,  $k_{21} = 2 \times 10^8 \text{ s}^{-1}$ . The results indicate that the fast migration of excitation energy brings about the quenching of the excited monomer state, and causes the efficient intramolecular excimer formation.

**KEY WORDS** Fluorescence / Kinetics / Time-Resolving Measurement / Intramolecular Excimer / Energy Migration / Trimer / Poly-(vinylnaphthalene-co-styrene) / Poly(2-vinylnaphthalene) /

Since the first observation of excimer emission in polystyrene,<sup>1</sup> many spectroscopic investigations of vinyl aromatic polymers have been reported, *e.g.*, poly(vinylnaphthalene),<sup>2</sup> poly(vinylcarbazole),<sup>3</sup> and poly(vinylpyrene).<sup>4</sup> In dilute solutions, these polymers show efficient intramolecular excimer formation with the pendant chromophores on the polymer chain. The excimer formation in the polymers is a thermally activated process controlled by the micro-Brownian motion of the skeletal chain. In solid films, it is also said that the energy migration between chromophores plays an important role in the excimer formation, since efficient excimer formation is observed in spite of the restriction of segmental motions in films.<sup>5</sup> Some workers<sup>6</sup> include the energy migration process in the general kinetic scheme of the photophysical processes, in dilute solutions as well as in films. But, a detailed mechanism has not been clarified yet. This is mainly due to the complexity of the polymer systems.

Photoluminescence properties of various copolymers of vinyl aromatic polymers have been investigated by many workers,<sup>7,8</sup> and their experimental data suggest the effective migration of excitation energy in films and in solutions.<sup>8</sup> In random or alternative copolymers, the migration process seems

to be interrupted by the insertion of photophysically inert species on the polymer chain, and even if the migration takes place in the polymers, it occurs mainly between non-adjacent chromophores within the domain of the copolymers. Under such conditions, it is expected that the migration and excimer formation processes become easily distinguishable.

In the present paper, the photoluminescence behavior of the copolymers of 2-vinylnaphthalene with styrene is investigated by photostationary and time-resolving measurements, in order to elucidate the interaction between adjacent chromophores and also between non-adjacent chromophores in a polymer chain. The observed luminescence behavior with energy migration has been interpreted by kinetic treatment. This analysis provides a quantitative understanding of the relationship between energy migration and the excimer formation in polymer systems.

### EXPERIMENTAL

#### *Materials*

2-Vinylnaphthalene (VN)–styrene random copolymers were prepared by radical polymerization

at 60°C using  $\alpha,\alpha'$ -azobisisobutyronitrile as the initiator. The polymerization was stopped at the conversion below 5%. The obtained polymer was reprecipitated several times from a benzene solution into methanol. The copolymer composition was determined by IR spectra, using bands at 820, 690, and 470  $\text{cm}^{-1}$ . The relationship between the composition of copolymer  $F$  and the composition of the starting monomer mixture  $f$ , is given in Figure 1. The following monomer reactivity ratios were obtained:  $r_{\text{VN}}=1.43$ ,  $r_{\text{styrene}}=0.53$ . These ratios agree with the values reported by Price *et al.*<sup>9</sup> Triad probabilities of naphthalene units in the copolymer chain,  $P_{\text{SNS}}$ ,  $P_{\text{SNN}}$ , and  $P_{\text{NNN}}$  (subscripts N and S refer to the vinyl naphthalene and styrene units, respectively) were estimated from these reactivity ratios. Molecular weights of the copolymers were determined by a calibrated GPC. The characteristics of these copolymers are summarized in Table I.

Trimer model compounds were synthesized as follows.

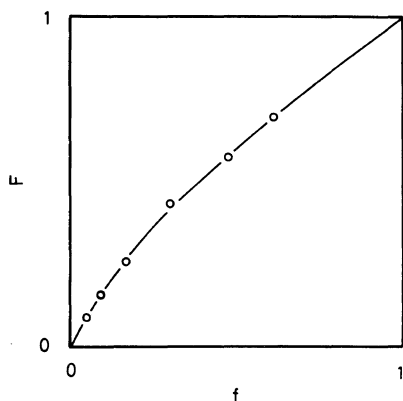


**Figure 1.** Copolymer composition curve of VN with styrene;  $F$  and  $f$  are the mole fractions of VN units in the copolymers and in monomer feeds, respectively.

1,5-Di(2-naphthyl)-3-phenylpentane (1,5-DN-3-PhPe): 1,5-dinaphthyl-3-pentanone obtained by aldol addition of 2-naphthaldehyde to acetone was reacted with phenyl magnesium bromide in ether solution. The product was recrystallized from cyclohexane to give the colorless crystalline 1,5-dinaphthyl-3-phenylpentan-3-ol: mp 120–121°C. The pentanol thus obtained was reduced in an acetic acid solution by the addition of zinc dust. The product was purified by column chromatography on silica gel: IR (KBr) 3050, 2940, 1630, 1600, 1510, 820, 740, 700, and 475  $\text{cm}^{-1}$ .

*Anal.* Calcd for  $\text{C}_{31}\text{H}_{28}$ : C, 92.95; H, 7.05%; M, 400. Found: C, 92.85; H, 6.91%;  $M^+$ , 400.

1,3,5-Tri(2-naphthyl)pentane (1,3,5-TNPe) was synthesized by the same method as that for 1,5-DN-3-PhPe. 2-Bromonaphthalene was used instead of bromobenzene. After purification by chromatography on silica gel, a colorless oily product was obtained: IR (KBr) 3050, 2940, 1630, 1600, 1500, 815, 740, and 475  $\text{cm}^{-1}$ ; NMR ( $\text{CS}_2$ )  $\delta$  1.95–2.30 (4H, m), 2.46–2.90 (5H, m), and 7.0–7.8 ppm (21H, m).

*Anal.* Calcd for  $\text{C}_{35}\text{H}_{30}$ : C, 93.29; H, 6.71%; M, 450. Found: C, 93.49; H, 6.99%;  $M^+$ , 450.

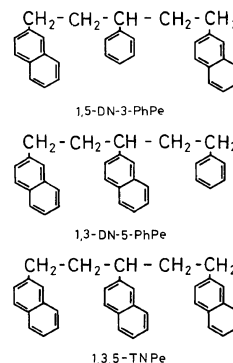


**Figure 2.** Structure of trimer model compounds.

**Table I.** Characteristics of vinyl naphthalene–styrene copolymers

Sample	$f$	$F$	Conversion/%	$M_w/10^4$	$P_{\text{NNN}}$	$P_{\text{SNN}}$	$P_{\text{SNS}}$
C1	0.05	0.09	2.9	18	0.006	0.15	0.85
C2	0.09	0.16	5.3	18	0.02	0.23	0.75
C3	0.17	0.26	2.3	21	0.05	0.34	0.62
C4	0.30	0.44	3.9	27	0.17	0.48	0.35
C5	0.47	0.58	3.3	34	0.31	0.49	0.20
C6	0.61	0.70	4.7	25	0.47	0.43	0.10

1,3-Di(2-naphthyl)-5-phenylpentane (1,3-DN-5-PhPe) was synthesized by the method described in ref 10. The molecular structures of these trimer model compounds are shown in Figure 2.

#### Measurements

All measurements were carried out in deaerated THF solutions, and the concentrations for the naphthalene chromophore were adjusted to *ca.*  $10^{-4}$  mol dm $^{-3}$ , at which intermolecular excimer formation is negligible. Absorption spectra were obtained with a Shimadzu UV-200S spectrophotometer, and fluorescence spectra with a Shimadzu spectrofluorophotometer model RF-502 in which the spectra were corrected for instrumental response. The quantum yields of emission were determined relative to that of quinine sulfate in 1 mol dm $^{-3}$  sulfuric acid, whose reported quantum yield is 0.51.<sup>11</sup> The decay curves of fluorescence were measured by a single photon counting technique (Ortec Inc., 9200 nanosecond fluorescence spectrometer). The half-width of the light pulse is *ca.* 2.5 ns. The monomer and excimer fluorescence were separated by a suitable combination of filters. A quartz dewar equipped with a thermocouple was used for low temperature measurements.

## RESULTS AND DISCUSSION

#### Photophysical Properties

Photostationary and transient measurements were carried out with the excitation of naphthalene chromophores. In these measurements, the phenyl groups were photophysically inert because of the excitation wavelength: 276 nm for photostationary measurements or 293 nm for the time-resolved measurements. At these excitation wavelengths, no phenyl groups absorb the exciting light, but the naphthalene chromophore is excited efficiently because of the large extinction coefficient. Fluorescence spectra are shown in Figure 3. The monomer fluorescence intensity at a wavelength of about 330 nm decreases with an increase in the naphthalene content in the copolymers. However, the excimer emission at around 400 nm increases. In Figures 4 and 5, the quantum yields of the monomer fluorescence,  $\Phi_M$  and the excimer fluorescence,  $\Phi_D$  are plotted against the probability that an excited naphthalene chromophore has an adjacent naphthyl group, *i.e.*,  $P_{SNN} + P_{NNN} = 1 - P_{SNS}$ .

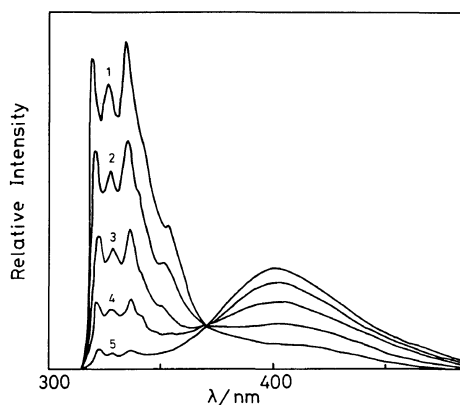


Figure 3. Fluorescence spectra of VN-styrene copolymers at 25°C: (1) C1; (2) C2; (3) C3; (4) C4; (5) PVN.

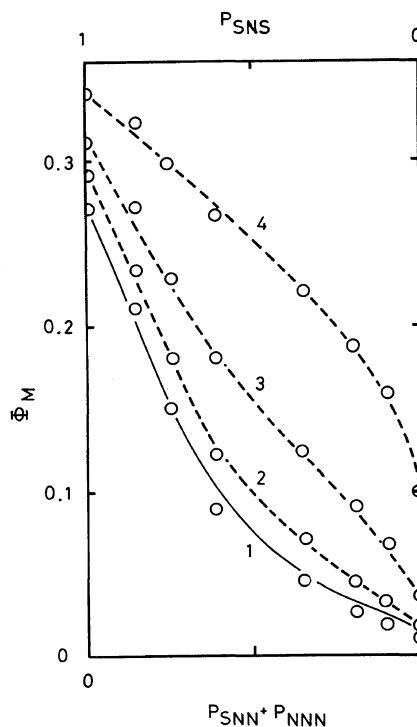


Figure 4. Quantum yield of monomer fluorescence at various temperatures: (1) 25°C; (2) 5°C; (3) -20°C; (4) -50°C. The solid line shows values calculated by eq 16-20.

Going on the assumption that isolated naphthalene units situated in the local sequence of SNS do not make any contribution to the intramolecular excimer formation in the copolymers, and that the

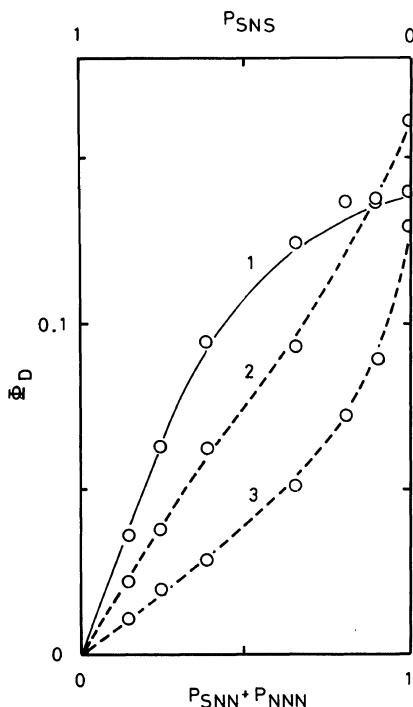


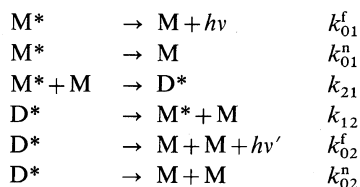
Figure 5. Quantum yield of excimer fluorescence at various temperatures: (1) 25°C; (2) -20°C; (3) -50°C. The solid line shows values calculated by eq 16-20.

excimer formation efficiencies in the sequence of SNN and NNN are not distinguishable, the quantum yields,  $\Phi_M$  and  $\Phi_D$  may be expressed as follows

$$\Phi_M = P_{SNS}\phi_M + (1 - P_{SNS})\phi'_M \quad (1)$$

$$\Phi_D = (1 - P_{SNS})\phi'_D \quad (2)$$

where  $\phi_M$  is the fluorescence quantum yield of the isolated naphthalene units, and  $\phi'_M$ ,  $\phi'_D$  refer to the quantum yields of the monomer fluorescence and the excimer fluorescence, respectively, for the non-isolated naphthyl groups. Here, the kinetic scheme for the dissipation process of excitation energy is written as follows



where M and M\* represent the ground state and the excited state of the monomer, respectively, and D\*

is the excimer state. The quantum yields,  $\phi_M$ ,  $\phi'_M$ , and  $\phi'_D$  are written by kinetic rate constants as follows

$$\phi_M = k_{01}^f / (k_{01}^f + k_{01}^n) \quad (3)$$

$$\phi'_M = k_{01}^f k_{21} / (k_1 k_2 - k_{21} k_{12}) \quad (4)$$

$$\phi'_D = k_{02}^f k_{21} / (k_1 k_2 - k_{21} k_{12}) \quad (5)$$

where

$$k_1 = k_{01}^f + k_{01}^n + k_{21} \quad (6)$$

$$k_2 = k_{02}^f + k_{02}^n + k_{12} \quad (7)$$

Equations 1 and 2 imply that both  $\Phi_M$  and  $\Phi_D$  should have linear relationships with the probability  $P_{SNN} + P_{NNN} (= 1 - P_{SNS})$ . However, neither of the obtained results are in accordance with these simple linear relationships as shown in Figures 4 and 5. At low temperatures, as the content of naphthalene chromophore increases,  $\Phi_M$  decreases particularly in the high content region, and intramolecular excimers are formed more efficiently than expected by the above relationships. At high temperatures, the monomer fluorescence is quenched notably even in the relatively low content of naphthyl groups. These facts indicate that the isolated naphthalene chromophores on the polymer chain also contribute to the intramolecular excimer formation. This was confirmed by the measurements of emission decays using a single photon counting technique.

Figure 6 shows the decay curves  $I_M(t)$  of the monomer fluorescence for various copolymers after excitation by a pulse having a half-width of about 2.5 ns. For the copolymers of low naphthalene content, the obtained  $I_M(t)$ 's show simple exponential decays, but their lifetimes are 48, 38, and 28 ns for C1, C2, and C3, respectively. These lifetimes are shorter than that of the monomeric compound, 2-ethylnaphthalene (MNEt) under the same condition: 54 ns. If the isolated excited naphthalene chromophores situated in the sequence of SNS, play no role in the excimer formation and dissipate to the ground state with their intrinsic rate constant  $k_{01} (= k_{01}^f + k_{01}^n)$ , the component of this corresponding lifetime, 54 ns should be observed within the decay curves of those copolymers as follows

$$I_M(t) \propto P_{SNS} \exp(-k_{01}t) + C(1 - P_{SNS})\{\exp(-\lambda_1 t) + A \exp(-\lambda_2 t)\} \quad (8)$$

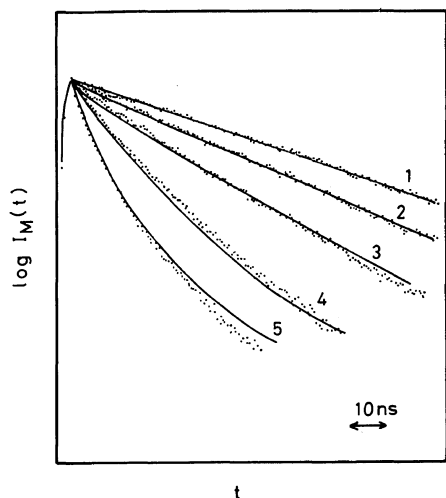


**Figure 6.** Decay curves of monomer fluorescence for the copolymers (1) C1, (2) C2, (3) C3, (4) C4, and (5) C5. The solid lines are the curves calculated by eq 16–20 and 23.

where  $C$  is a constant. Thus, the results obtained in Figure 6 show that the isolated excited naphthalene units are intramolecularly quenched in solution. These phenomena suggest the effective diffusion of naphthalene units or the excitation energy in the polymer molecules. For copolymers of high naphthalene content, the observed decays of  $I_M(t)$  consist of two or more components, indicating the contribution of the excimer dissociation process.

The decay curves of the excimer fluorescence  $I_D(t)$  for poly(2-vinylnaphthalene) (PVN) and various copolymers are shown in Figure 7. It can be noted that the rise of excimer emission for the copolymers of low naphthalene content is much slower than that of PVN. For example, the rise time of C1's excimer emission is estimated to be apparently *ca.* 11 ns, although some components of faster rise time than this are observed in the decay curve. The composition of naphthalene units in C1 is only 9%, but the evaluated value for the probability of  $P_{SNN}$  is about 15%. The predominant portion of the excimer fluorescence of C1 can be reasonably assumed to be emitted from the excimer formed between such adjacent naphthalene units. The relatively slow rise time for the copolymers thus suggests that the segment motion controlling the excimer formation in the polymer chain is considerably slower than the value expected from the  $k_{21}$  for homopolymer PVN:

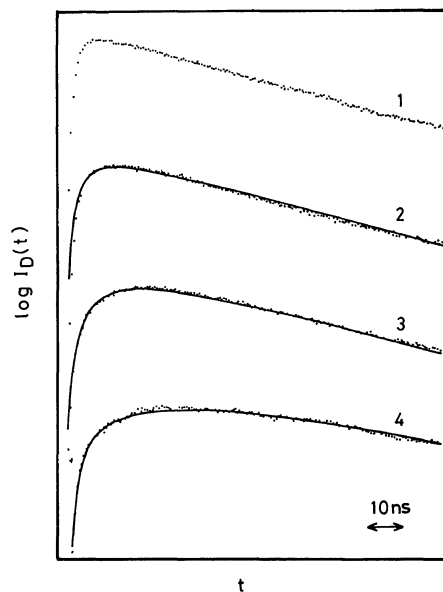


**Figure 7.** Decay curves of the excimer fluorescence for the copolymers: (1) PVN; (2) C6; (3) C4; (4) C2. The solid lines are the curves calculated by eq 16–20 and 23.

$k_{21}(\text{PVN}) = 7 \times 10^8 \text{ s}^{-1}$  at 25°C. The excimer formation processes in the copolymers are complex, and a more detailed quantitative discussion must be made on the basis of kinetic rate equations. Later on in this paper, kinetic treatment will demonstrate that the slow rise time is due to the process of intramolecular energy migration from the isolated naphthalene to the paired naphthalene chromophore. Before such kinetic treatment, it was necessary to clarify the characteristics of excimer formation in the local sequence of copolymer chains. For this purpose, three kinds of trimer model compounds were synthesized and their photophysical properties examined.

#### Excimer Formation in Trimer Model Compounds

Fluorescence spectra are shown in Figure 8. Although the absorption spectra of these trimers are essentially identical, the fluorescence spectra are considerably different with each other. There is no emission of intramolecular excimers in the compound, 1,5-DN-3-PhPe. But efficient intramolecular excimer formation is observed for 1,3-DN-5-PhPe and 1,3,5-TNPe. The monomer fluorescence band and the excimer emission band are the same in these compounds. The temperature dependence of

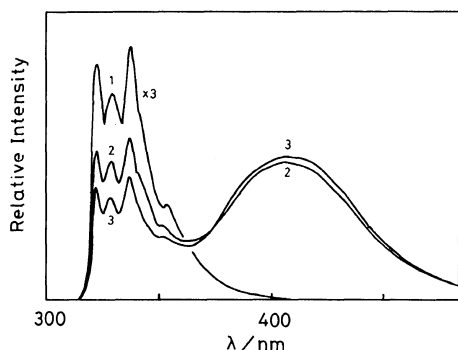


Figure 8. Fluorescence spectra of trimer model compounds at  $-20^{\circ}\text{C}$ : (1) 1,5-DN-3-PhPe; (2) 1,3-DN-5-PhPe; (3) 1,3,5-TNPe.

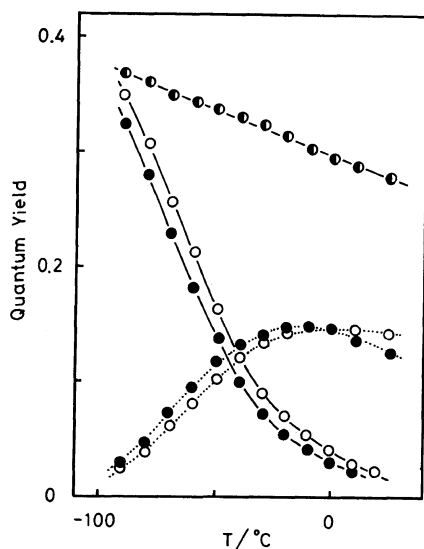


Figure 9. Temperature dependence of the quantum yields  $\Phi_M$  (—) and  $\Phi_D$  (·····): (●) 1,5-DN-3-PhPe; (○) 1,3-DN-5-PhPe; (●) 1,3,5-TNPe.

the quantum yields for the monomer and excimer fluorescence are shown in Figure 9. 1,5-DN-3-PhPe shows no indication of the excimer formation throughout the whole temperature range, as is also the case for 1,5-dinaphthylpentane.<sup>12</sup> The quantum yield of the monomer fluorescence and its lifetime agree with those of 2-ethylnaphthalene (MNEt), which can be regarded as a monomeric naphthalene unit of trimers and copolymers. Thus, the excited naphthyl groups of 1,5-DN-3-PhPe behave like isolated chromophores. This indicates that the intramolecular excimer is formed only between ad-

jacent chromophores in the trimer model compound, 1,3,5-TNPe.

As shown in Figure 9, efficient intramolecular excimer formation is observed for 1,3-DN-5-PhPe and 1,3,5-TNPe. The ratios of the excimer fluorescence quantum yield ( $\Phi_D$ ) to the monomer fluorescence quantum yield ( $\Phi_M$ ) can be regarded as the value proportional to the excimer formation rate constant under the condition of low temperature. 1,3,5-TNPe shows a higher efficiency of excimer formation than 1,3-DN-5-PhPe, although the equilibrium conformation and its rotational relaxation processes seem little affected by the change in the molecular structure, from the naphthyl group to the phenyl group at the one end of the trimer model compounds.

In order to clarify the fluorescence behavior, individual rate constants in the photophysical kinetic scheme were determined by measuring the rise and decay curves for excimer fluorescence. Going on the assumption that the actual lifetime of the monomer emission in the absence of the excimer formation process is equal to the lifetime of MNEt under the same conditions, all rate constants can be determined as follows.

The theoretical response functions,  $F_M(t)$  and  $F_D(t)$  for the monomer and excimer fluorescence, are derived as

$$F_M(t) = C_M \{ \exp(-\lambda_1 t) + A \exp(-\lambda_2 t) \} \quad (9)$$

$$F_D(t) = C_D \{ \exp(-\lambda_1 t) - \exp(-\lambda_2 t) \} \quad (10)$$

where  $C_M$ ,  $C_D$ ,  $A$ ,  $\lambda_1$ , and  $\lambda_2$  are rate constant functions.

$$\lambda_{1,2} = [k_1 + k_2 \mp \{(k_1 - k_2)^2 + 4k_{21}k_{12}\}^{1/2}] / 2 \quad (11)$$

With the assumption above mentioned, the rate constants,  $k_{01}^f$  and  $k_{01}^n$  are determined from measurements of quantum yield and the lifetime of MNEt. Thus, the other rate constants,  $k_{21}$ ,  $k_{12}$ ,  $k_{02}^f$ , and  $k_{02}^n$  can be obtained from the observed values,  $\lambda_1$ ,  $\lambda_2$ ,  $\Phi_M$ , and  $\Phi_D$  by using the following

$$\Phi_M = k_{01}^f k_2 / \lambda_1 \lambda_2 \quad (12)$$

$$\Phi_D = k_{02}^f k_{21} / \lambda_1 \lambda_2 \quad (13)$$

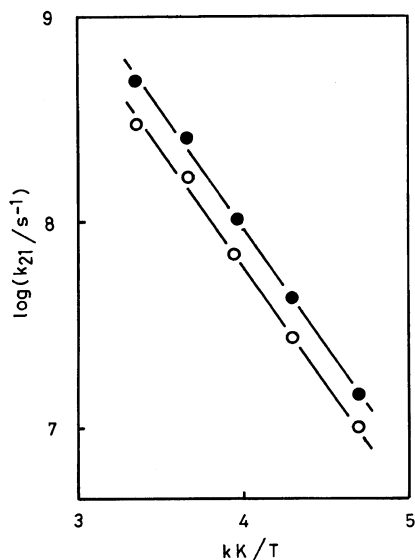
$$\lambda_1 + \lambda_2 = k_1 + k_2 \quad (14)$$

$$\lambda_1 \lambda_2 = k_1 k_2 - k_{21} k_{12} \quad (15)$$

The difference in the rate constants for 1,3-DN-5-PhPe and 1,3,5-TNPe occurs mainly in regard to

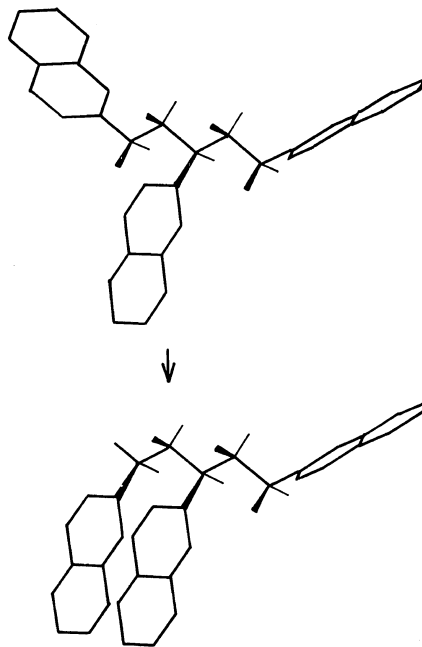
**Table II.** Excimer formation rate constant of trimer model compounds

$T/^\circ\text{C}$	$k_{21}/10^7 \text{ s}^{-1}$	
	1,3-DN-5-PhPe	1,3,5-TNPe
25	29.	49.
0	17.	26.
-20	7.0	10.
-40	2.8	4.4
-60	1.0	1.4

**Figure 10.** Arrhenius plot of the intramolecular excimer formation rate constant  $k_{21}$  for the trimer model compounds: (○) 1,3-DN-5-PhPe; (●) 1,3,5-TNPe.

rate constants,  $k_{21}$  and these values are listed in Table II. Here, the rates  $k_{21}$  for 1,3,5-TNPe are 1.4–1.6 times larger than those of 1,3-DN-5-PhPe. The other rate constants for both trimers are quite similar although some difference is found in the dissociation rate constants. The logarithms of  $k_{21}$  against the reciprocal of temperature are plotted in Figure 10. The activation energy for the excimer formation process is given as the slope and was found to be almost the same value,  $5.3 \text{ kcal mol}^{-1}$ . The obtained large formation rate for 1,3,5-TNPe is thus due to the increase in the frequency factor.

The equilibrium conformation and the relaxation process in that portion of the skeletal chain linking two naphthalene chromophores are not seriously

**Figure 11.** Schematic figure of favorable conformational change for excimer formation in trimer model compounds.

affected by changing the kind of terminal chromophore from naphthyl to phenyl. Thus, the increase in the association rate constant can be explained on the basis of the following reasons: the excited naphthyl group in the middle of the trimer is capable of forming excimers with either terminal naphthyl group, although the excited naphthyl groups at the end of the trimer have the same probability as those of 1,3-DN-5-PhPe. Consequently, the efficiency of the intramolecular excimer formation in 1,3,5-TNPe becomes higher than that of 1,3-DN-5-PhPe. The association rate of one adjacent pair of naphthyl groups is determined by the internal rotation of the skeletal chain from the *trans* to the *gauche* form, as shown in Figure 11.<sup>10</sup> From the symmetry in the molecular structure, it can be reasonably assumed that the association rate  $k_{21}$  for the excited middle chromophore is twice as large as that for the excited terminal chromophores. If the excimer formation rate is averaged for one middle chromophore and two terminal chromophores of 1,3,5-TNPe, it becomes 4/3 times larger than that of 1,3-DN-5-PhPe. The observed rate constants at various temperatures were found

to be 1.4–1.6 times larger than those of 1,3-DN-5-PhPe, and somewhat larger than that predicted by the above discussion. The further increase in  $k_{21}$  is interpreted as the effect of extremely fast energy migration, compared with the conformational relaxation time. When the excitation energy is delocalized among chromophores by this fast migration rate, the association rate should be proportional to the probability that the excimer conformation is generated in either adjacent naphthalene pairs of the trimer, 1,3,5-TNPe. The association constant of 1,3,5-TNPe is thus doubled by the delocalization of excitation energy, as compared with 1,3-DN-5-PhPe. The somewhat larger observed values than those predicted seem to indicate such a delocalization effect.

#### Kinetic Treatments

From the observed quantum yields and decay profiles, the following two factors should be considered. First, intramolecular excimers are formed only between adjacent naphthalene chromophores on the polymer chain, and the excimer formation rate constant of the excited naphthyl groups situated in the sequence of NNN should be at least twice as large as that in the sequence of SNN. Secondly, energy migration occurs intramolecularly and averages the excitation energy dissipation processes, originally determined by the local sequence of the pendant naphthalene units. Here, by taking into account these two factors, the following steady state kinetic equations can be written

$$\begin{aligned} d[M_{\text{SNS}}^*]/dt = & P_{\text{SNS}}I_0 + k_i P_N P_{\text{SNS}}([M_{\text{SNN}}^*] + [M_{\text{NNN}}^*]) \\ & - \{k_{01} + k_i P_N (P_{\text{SNN}} + P_{\text{NNN}})\} [M_{\text{SNS}}^*] \end{aligned} \quad (16)$$

$$\begin{aligned} d[M_{\text{SNN}}^*]/dt = & P_{\text{SNN}}I_0 \\ & + k_i P_N P_{\text{SNN}}([M_{\text{SNS}}^*] + [M_{\text{NNN}}^*]) + k_{12}[D_{\text{SNN}}^*] \\ & - \{k_{01} + k_{21} + k_i P_N (P_{\text{SNS}} + P_{\text{NNN}})\} [M_{\text{SNN}}^*] \end{aligned} \quad (17)$$

$$\begin{aligned} d[M_{\text{NNN}}^*]/dt = & P_{\text{NNN}}I_0 \\ & + k_i P_N P_{\text{NNN}}([M_{\text{SNS}}^*] + [M_{\text{SNN}}^*]) \\ & + k_{12}[D_{\text{NNN}}^*] \\ & - \{k_{01} + 2k_{21} + k_i P_N (P_{\text{SNS}} + P_{\text{SNN}})\} [M_{\text{NNN}}^*] \end{aligned} \quad (18)$$

$$d[D_{\text{SNN}}^*]/dt = k_{21}[M_{\text{SNN}}^*] - (k_{12} + k_{02})[D_{\text{SNN}}^*] \quad (19)$$

$$d[D_{\text{NNN}}^*]/dt = 2k_{21}[M_{\text{NNN}}^*] - (k_{12} + k_{02})[D_{\text{NNN}}^*] \quad (20)$$

where  $M_{\text{SNS}}^*$ ,  $M_{\text{SNN}}^*$ , and  $M_{\text{NNN}}^*$  represent the singlet excited naphthalene units situated in the sequences of SNS, SNN, and NNN, respectively.  $k_i$  is the intramolecular transfer rate constant of the excitation energy from an excited naphthalene monomer to another naphthalene chromophore on the polymer chain,  $P_N$  is the composition of the VN unit in the copolymer, and  $P_N P_{\text{SNS}}$ ,  $P_N P_{\text{SNN}}$ , and  $P_N P_{\text{NNN}}$  represent the intramolecular concentration of the local sequences, SNS, SNN, and NNN, respectively. The notation of other rate constants is the same as that mentioned in the previous section, but the association rate constant,  $k_{21}$  refers to the excimer formation rate constant of the isolated dimer sequence NN on the polymer chain. This rate is thus closely related to the conformational changes in the polymer segments. By using the solutions of eq 16–20, the quantum yields  $\Phi_M$  and  $\Phi_D$  are given as

$$\Phi_M = k_{01}([M_{\text{SNS}}^*] + [M_{\text{SNN}}^*] + [M_{\text{NNN}}^*])/I_0 \quad (21)$$

$$\Phi_D = k_{02}([D_{\text{SNN}}^*] + [D_{\text{NNN}}^*])/I_0 \quad (22)$$

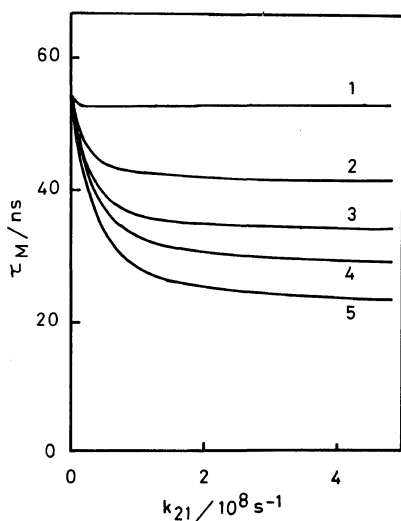
The decay curves of the monomer and the excimer emission,  $I_M(t)$  and  $I_D(t)$  are obtained by solving the differential equations which eliminate the excitation term  $I_0$ , from eq 16–20 under the following initial conditions:

$$\begin{aligned} [M_{\text{SNS}}^*]_0 = & P_{\text{SNS}}I_0 & [M_{\text{SNN}}^*]_0 = & P_{\text{SNN}}I_0 \\ [M_{\text{NNN}}^*]_0 = & P_{\text{NNN}}I_0 & [D_{\text{SNN}}^*]_0 = & [D_{\text{NNN}}^*]_0 = 0 \end{aligned}$$

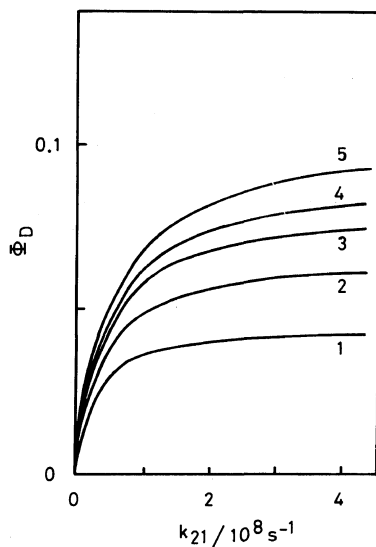
In these kinetic equations, several rate constants for the naphthalene chromophore have already been determined from measurements of various model compounds and polymers.<sup>10</sup> Thus, there are only two unknown parameters:  $k_i$  and  $k_{21}$ .

Figure 12 shows the lifetime of the monomer emission decay  $\tau_M$  calculated for various  $k_i$  values at  $P_{\text{SNS}}=0.7$ . For the low naphthalene content samples, the calculated decay curve of the monomer fluorescence,  $F_M(t)$  can be approximated to be single exponential function whose decay time represents the lifetime of an isolated naphthalene chromophore on the polymer chain. The decay time is governed mainly by the migration rate constant  $k_i$ , and hardly depends on the association rate constant,  $k_{21}$  in the region of  $10^8 \text{ s}^{-1}$ . The migration





**Figure 12.** Monomer fluorescence lifetime,  $\tau_M$  calculated for various values of  $k_{21}$  and  $k_i$ : (1)  $k_i = 1 \times 10^7 \text{ s}^{-1}$ ; (2)  $k_i = 1 \times 10^8 \text{ s}^{-1}$ ; (3)  $k_i = 2 \times 10^8 \text{ s}^{-1}$ ; (4)  $k_i = 3 \times 10^8 \text{ s}^{-1}$ ; (5)  $k_i = 5 \times 10^8 \text{ s}^{-1}$ .



**Figure 13.** Quantum yield,  $\Phi_D$  calculated for various values of  $k_{21}$  and  $k_i$ . Numerals represent the same  $k_i$  values as those in Figure 12.

process of excitation energy from an isolated SNS chromophore to an adjacent naphthalene pair, SNN or NNN, involves substantial quenching process of the excited monomer state  $M^*$ , since nearly all of the excitation energy in  $M_{SNN}^*$  and  $M_{NNN}^*$  flows in the corresponding excimer states, and scarcely

**Table III.** Photophysical rate constants obtained for VN-styrene copolymers

$k_{01}^f/10^7 \text{ s}^{-1}$	0.49
$k_{01}^n/10^7 \text{ s}^{-1}$	1.31
$k_{02}^f/10^7 \text{ s}^{-1}$	0.23
$k_{02}^n/10^7 \text{ s}^{-1}$	1.3
$k_{12}/10^7 \text{ s}^{-1}$	0.6
$k_{21}/10^7 \text{ s}^{-1}$	20.
$k_i/10^7 \text{ s}^{-1}$	30.

goes back to the isolated naphthalene chromophore, SNS. It is obvious from Figure 12 that the migration rates of  $2 \times 10^8 \text{ s}^{-1}$  or above must be used in order to reproduce the experimental data ( $\tau_M = 33 \text{ ns}$  at  $P_{SNS} = 0.7$ ). On the other hand, the emission properties of the excimers, *i.e.*, the quantum yield  $\Phi_D$  or the rise curve of excimer emission, are affected by the change in association rate constants over a wide range of  $k_{21}$ . Figure 13 shows the dependence of  $\Phi_D$  for various  $k_i$ 's. Appropriate values of  $k_{21}$  and  $k_i$  were chosen from Figures 12 and 13:  $k_{21} = 2 \times 10^8 \text{ s}^{-1}$ ,  $k_i = 3 \times 10^8 \text{ s}^{-1}$ . The agreement between calculated and observed values was examined for samples of various naphthalene content. All rate constants thus obtained are listed in Table III.

Figures 6 and 7 show the calculated decay curves for the  $I_M(t)$  and  $I_D(t)$ , respectively, which are given by the following equation

$$I(t) = \int_0^t p(t') F(t-t') dt' \quad (23)$$

where  $F(t)$  is the calculated response function from the differential equation, and  $p(t)$  is the exciting light pulse. These curves agree very well with the experimental curves over a wide range of naphthalene content. As mentioned above, the decay curve  $I_M(t)$  for the low naphthalene content region can be approximated by a single exponential function. Actually, the decay functions are given by the sum of five exponential terms as the solutions to eq 16–20. Here, we discuss the decay profile under the condition that the value of  $k_{12}$  is negligibly small. The decay curves of  $F_M(t)$  and  $F_D(t)$  can thus be expressed by the sums of three or four exponential terms, respectively, as follows

$$F_M(t) = \sum^3 A_{M,i} \exp(-t/\tau_i) \quad (24)$$

**Table IV.** Decay parameters of the monomer and excimer fluorescence for the low naphthalene content samples

C1 ( $P_{\text{SNS}}=0.85$ )				
	$i=1$	$i=2$	$i=3$	$i=4$
$\tau_i/\text{ns}$	46.	4.1	2.2	65.
$A_{\text{M},i}$	0.88	0.11	0.01	—
$A_{\text{D},i}$	-0.82	-0.17	-0.01	1.0
C2 ( $P_{\text{SNS}}=0.75$ )				
$\tau_i/\text{ns}$	35.	3.9	2.1	65.
$A_{\text{M},i}$	0.82	0.16	0.01	—
$A_{\text{D},i}$	-0.79	-0.19	-0.02	1.0

$$F_{\text{D}}(t) = \sum_{i=1}^4 A_{\text{D},i} \exp(-t/\tau_i) \quad (25)$$

The parameters in eq 24 and 25 are listed in Table IV for the samples of  $P_{\text{SNS}}=0.85$  and 0.75. The decay times,  $\tau_1$ ,  $\tau_2$ , and  $\tau_3$  are originally the decay times of the naphthalene chromophores at the sequences of SNS, SNN, and NNN, respectively, but the calculated decay times deviate from these values owing to the mixing of the energy dissipation processes. For the decay curve  $F_{\text{M}}(t)$ , the preexponential factor  $A_{\text{M},1}$  is dominant in eq 24, and the monomer emission thus shows a single exponential decay having the longest lifetime  $\tau_1$ , except for the time immediately following the exciting pulse. For the decay curve  $F_{\text{D}}(t)$ ,  $\tau_1$ ,  $\tau_2$ , and  $\tau_3$  become the rise time of the excimers, and the decay profiles of  $F_{\text{D}}(t)$  are considerably affected by the rise components,  $\tau_2$  and  $\tau_3$  not only for samples of high naphthalene content but also for those of low naphthalene content. The observed rise curves of  $I_{\text{D}}(t)$  can be simulated by using at least two or three of these rise components, but not by a single one.

Stationary state behavior was also examined using the eq 16–20, under the conditions,  $d[\text{M}^*]/dt = d[\text{D}^*]/dt = 0$  for the naphthalene chromophore of each sequence. In Figures 4 and 5, the solid lines show the quantum yields,  $\Phi_{\text{M}}$  and  $\Phi_{\text{D}}$ , calculated for various naphthalene content of copolymers. The rate constants used in this simulation are the same as those for the calculation of decay profile, and can be used to reproduce the observed quantum yields,  $\Phi_{\text{M}}$  and  $\Phi_{\text{D}}$  over a wide range of naphthalene content. Thus, kinetic equations provide a good representation of both the transient and steady state behavior of the copolymers, in spite of

their simplicity.

The kinetic equations indicate important characteristics of the polymer systems. The large value for the migration rate constant ( $k_1 = 3 \times 10^8 \text{ s}^{-1}$ ) shows a considerably fast migration of excitation energy among pendant chromophores on the polymer chain. It has been said that there are two main mechanisms in these singlet-singlet migration systems: Coulombic interaction between electronic excited states of chromophores and an exchange interaction between the overlapping electron clouds of the chromophores. The former Coulombic interaction usually operates within a longer distance of chromophores than that of the latter mechanism, but spectroscopic data for MNEt in THF gives *ca.* 1.2 nm as the critical distance,  $R_0$ , with the following equation for the dipole-dipole interaction<sup>13</sup>

$$R_0^6 = \frac{(9000 \ln 10) K^2}{128 \pi^5 n^4 N_0} \int_0^\infty f(\nu) \epsilon(\nu) d\nu/\nu^4 \quad (26)$$

where  $n$  is the solvent refractive index,  $K^2$  is an orientation factor,  $\epsilon(\nu)$  is the molar extinction coefficient at wavenumber  $\nu$  and  $f(\nu)$  is the relative donor fluorescence intensity at  $\nu$ . In a low viscosity medium satisfying the condition,  $R_0 \ll (2D\tau_{\text{M}})^{1/2}$ , the migration obeys Stern–Volmer kinetics.<sup>13</sup> The rate equation can thus be written by the time-independent migration rate constant,  $k_1$  and the concentration of energy acceptor, A as follows.

$$d[\text{M}^*]/dt = -(k_{01} + k_1[\text{A}])(\text{M}^*) \quad (27)$$

In eq 16–20, [A] is replaced by the intramolecular concentrations,  $P_{\text{N}}P_{\text{SNS}}$ ,  $P_{\text{N}}P_{\text{SNN}}$ , and  $P_{\text{N}}P_{\text{NNN}}$  for the corresponding naphthalene sequences in the polymer molecules. Here, the rate constant  $k_1$  is closely related to the Brownian motion of the polymer segments, since either migration mechanism operates only at a short distance: 1.2–1.5 nm, which can be regarded as an encounter distance of the chromophores on the polymer chain. In consideration of the fact that the migration probability per one collision,  $p$ , is equal to 0.5 for  $r < R_0$ , and  $p = 0$  for  $r > R_0$ ,<sup>14</sup> the experimental data indicate that the polymer segments collide with the other part of the same polymer chain at a rate of  $6 \times 10^8 \text{ s}^{-1}$ . Thus, the excitation energy migrates from one excited chromophore to another through the intramolecular collision of the polymer segments. It can be said that the mi-

gration process is assisted by the micro-Brownian motion of the polymer chain.

In a high content region of naphthalene chromophores or in that homopolymer, PVN, another migration process takes place in addition to the migration mentioned above. In such high naphthalene content samples, most of the naphthalene units are located within a row of consecutive chromophores on the polymer chain. The excitation energy migrates along this row of chromophores at a faster rate than that obtained by kinetic analysis. According to the quenching experiments for the monomer and excimer fluorescence of poly(vinyl-naphthalene-co-styrene),<sup>15</sup> the fast energy migration takes place at a naphthalene content above 40% (C4), at which a marked increase in quenching rate constants was observed for the monomer fluorescence.

Although the kinetic equations mentioned above should be applied only to samples of low naphthalene content, the calculated values are in good accordance with the experimental results in the wide range of naphthalene content. Thus, it is concluded that this kinetic model for the copolymers provides a good representation of the photophysical behavior. It may be said that key points of the photophysical processes can be understood by this kinetic treatment, in spite of the approximate nature of the treatment on complicated polymer systems.

## REFERENCES

1. L. J. Basile, *J. Chem. Phys.*, **36**, 2204 (1962).  
S. S. Yanari, F. A. Bovey, and R. Lumry, *Nature*, **200**, 242 (1963).
2. M. T. Vala, J. Haebig, and S. A. Rice, *J. Chem. Phys.*, **43**, 886 (1965).  
Y. Nishijima, *J. Polym. Sci., C*, **31**, 353 (1970).  
C. David, W. Demartean, and G. Geuskens, *Eur. Polym. J.*, **6**, 1397 (1970).  
L. A. Harrah, *J. Chem. Phys.*, **56**, 385 (1972).  
R. B. Fox, T. R. Price, R. F. Cozzens, and J. R. McDonald, *J. Chem. Phys.*, **57**, 534 (1972).  
C. David, M. Piens, and G. Geuskens, *Eur. Polym. J.*, **8**, 1019 (1972).  
Y. Nishijima, Y. Sasaki, M. Tsujisaki, and M. Yamamoto, *Rep. Prog. Polym. Phys. Jpn.*, **15**, 453 (1972).  
S. Ito, M. Yamamoto, and Y. Nishijima, *Rep. Prog. Polym. Phys. Jpn.*, **19**, 421 (1976).  
K. P. Ghiggino, R. D. Wright, and D. Phillips, *J. Polym. Sci., Polym. Phys. Ed.*, **16**, 1499 (1978).
3. W. Klöpffer, *J. Chem. Phys.*, **50**, 2337 (1969).  
P. C. Johnson and H. W. Offen, *J. Chem. Phys.*, **55**, 2945 (1971).  
C. David, M. Piens, and G. Geuskens, *Eur. Polym. J.*, **8**, 1291 (1972).  
Y. Nishijima, Y. Sasaki, K. Hirota, and M. Yamamoto, *Rep. Prog. Polym. Phys. Jpn.*, **15**, 449 (1972).  
G. E. Johnson, *J. Chem. Phys.*, **62**, 4697 (1975).  
M. Yokoyama, T. Tamamura, M. Atsumi, M. Yoshimura, Y. Shiota, and H. Mikawa, *Macromolecules*, **8**, 101 (1975).  
A. Itaya, K. Okamoto, and S. Kusabayashi, *Bull. Chem. Soc. Jpn.*, **49**, 2082 (1976).  
K. P. Ghiggino, R. D. Wright, and D. Phillips, *Eur. Polym. J.*, **14**, 567 (1978).  
C. E. Hoyle, T. L. Nemzek, A. Mar, and J. E. Guillet, *Macromolecules*, **11**, 429 (1978).  
M. Keyanpour-Rad, A. Ledwith, and G. E. Johnson, *Macromolecules*, **13**, 229 (1980).
4. J. R. McDonald, W. E. Echols, T. R. Price, and R. B. Fox, *J. Chem. Phys.*, **57**, 1746 (1972).  
M. Yokoyama, T. Tamamura, T. Nakano, and H. Mikawa, *Chem. Lett.*, 499 (1972).  
K. Hirota, M. Yamamoto, and Y. Nishijima, *Rep. Prog. Polym. Phys. Jpn.*, **16**, 509 (1973).
5. C. David, M. Piens, and G. Geuskens, *Eur. Polym. J.*, **9**, 533 (1973).  
C. W. Frank and L. A. Harrah, *J. Chem. Phys.*, **61**, 1526 (1974).  
C. W. Frank, M. A. Gashgari, *Macromolecules*, **12**, 163 (1979).
6. C. David, M. Lempereur, and G. Geuskens, *Eur. Polym. J.*, **9**, 1315 (1973).  
A. M. North, *Br. Polym. J.*, **7**, 119 (1975).  
J. S. Asper, C. E. Hoyle, and J. E. Guillet, *Macromolecules*, **11**, 925 (1978).  
R. F. Reid and I. Soutar, *J. Polym. Sci., Polym. Phys. Ed.*, **16**, 231 (1978).
7. Y. Nishijima, K. Mitani, S. Katayama, and M. Yamamoto, *Rep. Prog. Polym. Phys. Jpn.*, **13**, 425 (1970).  
F. Schneider and J. Springer, *Makromol. Chem.*, **146**, 181 (1971).  
R. B. Fox, T. R. Price, R. F. Cozzens, and J. R. McDonald, *J. Chem. Phys.*, **57**, 534 (1972).  
C. David, M. Lempereur, and G. Geuskens, *Eur. Polym. J.*, **9**, 1315 (1973).  
C. David, M. Piens, and G. Geuskens, *Eur. Polym. J.*, **12**, 621 (1976).
8. A. C. Somersall and J. E. Guillet, *Macromolecules*, **6**, 218 (1973).  
C. David, M. Piens, and G. Geuskens, *Eur. Polym. J.*, **9**, 533 (1973).  
R. B. Fox, T. R. Price, R. F. Cozzens, and W. H. Echols, *Macromolecules*, **7**, 937 (1974).  
M. Yokoyama, T. Tamamura, T. Nakano, and H.

- Mikawa, *J. Chem. Phys.*, **65**, 272 (1976).  
C. David, N. P. Lavarelle, and G. Geuskens, *Eur. Polym. J.*, **13**, 15 (1977).  
R. F. Reid and I. Soutar, *J. Polym. Sci., Polym. Phys. Ed.*, **16**, 231 (1978).  
R. F. Reid and I. Soutar, *J. Polym. Sci., Polym. Phys. Ed.*, **18**, 457 (1980).
9. C. C. Price, B. D. Halpern, and S. T. Voong, *J. Polym. Sci.*, **11**, 575 (1953).
  10. S. Ito, M. Yamamoto, and Y. Nishijima, *Bull. Chem. Soc. Jpn.*, **54**, 35 (1981).
  11. W. H. Melhuish, *J. Phys. Chem.*, **65**, 229 (1961).
  12. S. Ito, M. Yamamoto, and Y. Nishijima, *Rep. Prog. Polym. Phys. Jpn.*, **22**, 453 (1979).
  13. J. B. Birks, "Photophysics of Aromatic Molecules," Wiley-Interscience, London, 1970, Chapter 11.
  14. R. Voltz, G. Laustriat, and A. Coche, *J. Chim. Phys.*, **63**, 1253 (1966).
  15. S. Ito, M. Yamamoto, and Y. Nishijima, *Rep. Prog. Polym. Phys. Jpn.*, **23**, 543 (1980).